Oncogene (2014) **33,** 5173–5182

www.nature.com/onc

ORIGINAL ARTICLE

MicroRNAs, miR-154, miR-299-5p, miR-376a, miR-376c, miR-377, miR-381, miR-487b, miR-485-3p, miR-495 and miR-654-3p, mapped to the 14q32.31 locus, regulate proliferation, apoptosis, migration and invasion in metastatic prostate cancer cells

A Formosa[1,2], EK Markert[3], AM Lena[1], D Italiano[1], E Finazzi-Agro'[1], AJ Levine[3], S Bernardini[1], AV Garabadgiu[4], G Melino[1,2] and E Candi[1]

miRNAs act as oncogenes or tumor suppressors in a wide variety of human cancers, including prostate cancer (PCa). We found a severe and consistent downregulation of miRNAs, miR-154, miR-299-5p, miR-376a, miR-376c, miR-377, miR-381, miR-487b, miR-485-3p, miR-495 and miR-654-3p, mapped to the 14q32.31 region in metastatic cell lines as compared with normal prostatic epithelial cells (PrEC). In specimens of human prostate (28 normals, 99 primary tumors and 13 metastases), lower miRNA levels correlated significantly with a higher incidence of metastatic events and higher prostate specific antigen (PSA) levels, with similar trends observed for lymph node invasion and the Gleason score. We transiently transfected 10 members of the 14q32.31 cluster in normal prostatic epithelial cell lines and characterized their affect on malignant cell behaviors, including proliferation, apoptosis, migration and invasion. Finally, we identified FZD4, a gene important for epithelial-to-mesenchymal transition in (PCa), as a target of miR-377.

Oncogene (2014) **33,** 5173–5182; doi:10.1038/onc.2013.451; published online 28 October 2013

Keywords: microRNAs; prostate cancer; metastasis

INTRODUCTION

Prostate cancer (PCa) continues to burden the Western world with its high rates of incidence and mortality[1] despite the improved clinical detection and management of the disease due to techniques such as prostate-specific antigen (PSA) analysis, biopsy and the Gleason score. Thus, novel means to assess the presence of PCa, monitor its progression and predict its outcome are required, which necessitate a better understanding of its underlying molecular processes.

MicroRNAs (miRNAs) pose as attractive molecules in the advancement of cancer diagnostics and therapeutics.[2–7] These short non-coding RNA molecules negatively regulate the translation of target mRNA species by binding to their 3′ untranslated region (3′UTR). Over 1 000 human miRNA species are postulated to exist, and their role as oncogenes or tumor suppressors in a wide variety of human cancers, including PCa, has been well-documented.[8–11] Accordingly, we have identified miR-205 as a p63 target, which is able to inhibit PCa migration *in vitro* and metastasis *in vivo*.[12] This pathway can be inhibited by mutant p53, although in other tumors, such as pancreatic cancer, mutant p53 also seems to activate alternative mechanisms to induce metastasis (Muller and Melinopersonal observation). In contrast, miR-203 targeting p63 and other cytoskeleton-associated mRNAs also control proliferation, migration and invasive potential in (PCa) cells.[11,13,14] MiRNAs are often associated in clusters in the genome,[15] and several studies have shown a role for clustered miRNAs in cancer, whereby members of a cluster affect similar outcomes in tumorigenesis. The miR-17-92 cluster, for example, is recognized as oncogenic,[16] whereas the miR-15a and miR-16 clusters act as tumor suppressors by targeting multiple oncogenes such as BCL2, MCL1, CCND1 and WNT3A.[17]

Nearly a decade ago, 46 potential miRNA genes located in the human-imprinted 14q32 domain were identified through a computer-assisted approach, 40 of which were organized as a large cluster.[15] The 14q32 domain, termed *Dlk1-Gtl2* in mice or Dlk-Dio3 in humans, has an important role in development as revealed by the severe phenotypes observed in mice and humans associated with the alteration of genes within the region.[18] The expression of this cluster has been implicated in human malignancies including melanoma,[19] ependymoma,[20] osteosarcoma,[21] neuroblastoma,[22] hepatocellular carcinoma,[23] gastrointestinal stromal tumors,[23] ovarian cancer,[24] uterine osteosarcoma[25] and gliomas.[26] Some studies have revealed a tumor-suppressive function for a subset of miRNAs of the cluster, such as their pro-apoptotic effect in tumor cells,[21,27–30] and the anti-proliferative and anti-migratory role of miR-376 and -376c in melanoma cells.[19,31–33]

In a recent study, we quantified 750 human miRNAs for their expression in normal prostate epithelial cells (PrEC) and metastatic cell lines by means of an RT-pre-amp-qPCR array to identify miRNAs silenced by DNA methylation in human PCa.[34] We re-analyzed this array in search of potential tumor-suppressor miRNAs in PCa and found a severe and consistent downregulation of miRNAs mapped to the 14q32.31 region in metastatic cell lines as compared with PrEC. In the present study, we have analyzed the expression of 14q32.31 miRNAs in human PCa and found a downregulation of the cluster particular to metastatic samples. To ascertain the cellular function of 14q32.31 miRNAs, we transiently

[1]University of Tor Vergata, Department Experimental Medicine and Surgery, Rome, Italy; [2]IDI-IRCCS, Rome, Italy; [3]The Simons Center for Systems Biology, Institute for Advanced Study, Princeton, NJ, USA and [4]Laboratory of Molecular Pharmacology, Saint-Petersburg Technological Institute, 26 Moskovsky Prospect, Petersburg, Russia. Correspondence: Dr E Candi, University of Tor Vergata, Department Experimental Medicine and Surgery, via Montpellier 1, Rome 00133, Italy.
E-mail: candi@uniroma2.it
Received 10 May 2013; revised 24 July 2013; accepted 9 August 2013; published online 28 October 2013

transfected 10 members of the cluster in PCa cell lines and characterized their affect on malignant cell behaviors including proliferation, apoptosis, migration and invasion. Finally, we identified FZD4–a gene important for epithelial-to-mesenchymal transition in PCa—as a target of miR-377.

RESULTS

Expression of 14q32.31 miRNAs are downregulated in human prostate cancer

The chromosomal region 14q32.31 contains a large cluster of 42 intergenic miRNAs located within 10 kb of each other (Figure 1a). In our previous study,[34] we analyzed the expression of 650 miRNAs by megaplex stem-loop RT-qPCR on four cell lines: PrEC, PC3 (PCa metastasis to bone), DU145 (PCa metastasis to brain) and LNCaP (PCa metastasis to lymph nodes). As shown in Figure 1b, miRNAs mapped to the 14q32.31 region had a markedly lower expression in all tumorigenic cell lines as compared with PrEC. The only exception to this pattern was the fourfold increased expression of miR-494 and miR-656 in PC3 cells. To determine whether the expression pattern of 14q32.31 miRNAs in PCa cell lines manifested itself in human prostate specimens, we extracted miRNA data on 28 normal tissues, 99 primary tumors and 13 metastases from the GSE21032 data set by Taylor *et al.* available at the GEO website.[34] The data set comprised 17 miRNAs from the 14q32.31 region: miR-134, miR-154, miR-299-5p, miR-300, miR-376a, miR-376b, miR-376c, miR-377, miR-379, miR-381, miR-382, miR-409-3p, miR-485-3p, miR-487b, miR-494, miR-495 and miR-654-3p. Thirteen miRNAs showed clear downregulated expression trends in going from normal to localized tumor to metastatic cases

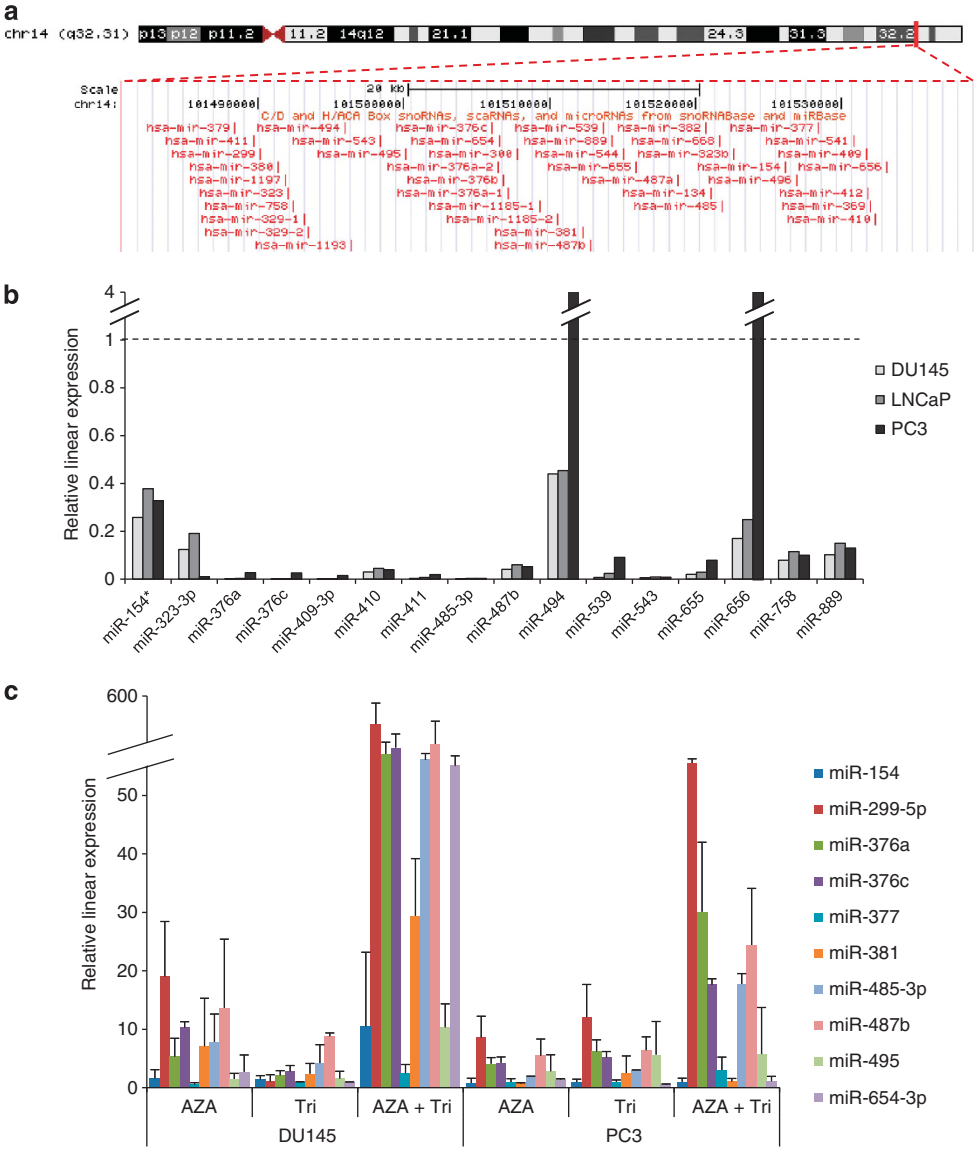

Figure 1. Expression of 14q32.31 miRNAs in PCa cell lines. (**a**) Screenshot (http://genome.ucsc.edu; GRCh37/hg19 assembly) of the region of interest at the chromosomal level (red horizontal bar, top image) and in detail (bottom image) showing the 42 miRNAs located within 10 kb of each other.[35] (**b**) Basal expression level by megaplex stem-loop RT-qPCR[34] of 14q32.31 miRNAs in PCa metastatic cell lines relative to the normal epithelial cell line PrEC (set to 1, dashed line). This graph was generated from our previously published data set[34] whereby a screening procedure using megaplex stem-loop qPCR was used to visualize the expression of 650 miRNAs across prostate cell lines (one biological replicate). Data normalization was carried out as previously described[34] (**c**) Treatment with the epigenetic drugs AZA and Trichostatin (Tri) causes the re-expression of several 14q32.31 miRNAs in DU145 and PC3 cells, with the greatest effect seen in DU145 upon dual treatment. Data are relative to control cells (set to 1) for the given cell line. The average of three independent experiments is shown. Error bars represent their standard deviation.

(Supplementary Figure S1a and S1b), 10 of which were statistically significant (miR-154, miR-299-5p, miR-376a, miR-376c, miR-377, miR-381, miR-487b, miR-485-3p, miR-495 and miR-654-3p). These 10 miRNAs, referred to as '14q32.31 miRNAs' from here on, were studied in greater detail as described next.

Epigenetic silencing contributes to diminished 14q32.31 miRNA expression in PCa cell lines

The close vicinity of 14q32.31 miRNAs coupled with their coordinated expression in PCa cell lines (Figure 1b) and human specimens (Supplementary Figure S1) suggested a transcriptional silencing mechanism responsible for the cluster's downregulation in tumorigenesis. Using the cBio Cancer Genomics portal,[35,36] we visualized DNA copy-number data on 14q32.31 miRNAs from the data set by Taylor *et al.* but found no alterations (data not shown). Hence, we hypothesized an epigenetic means of silencing for the cluster, especially given previous reports on its re-expression in cancer cells with epigenetic modifying drugs.[19,24] To this end, PC3 and DU145 cells were treated separately and in combination with the DNA-demethylating agent 5-aza-2′-deoxycytidine (AZA) and the histone deacetylase inhibitor Trichostatin A. Expression changes for the ten 14q32.31 miRNAs of interest were then analyzed by RT-qPCR. Figure 1c illustrates a modest upregulation of the miRNAs with either AZA or Trichostatin A and a marked increase in their expression (albeit miRNA and cell line-dependent) with dual-drug treatment. Taken together, these *in vitro* results demonstrate an important epigenetic contribution to the widespread downregulation of 14q32.31 miRNAs; however, an as-yet-unknown mechanism also participates in regulating the cluster's expression.

Expression of 14q32.31 miRNAs in human prostate cancer correlates with clinical and pathological variables

We analyzed the expression of 14q32.31 miRNAs in relation to various clinical parameters using the data set by Taylor *et al.*[35] miRNA expression data were available for 1 cell line (Vcap), 28 normal prostate tissue samples and 112 tumors including 13 metastases. The 14q32.31 miRNAs were combined into one gene signature and their concordant expression was measured using gene set enrichment analysis on the miRNA data.[36] Samples were delegated into low-, intermediate- and high-expression groups by clustering the resulting signature scores into three groups as shown by the heatmap in Figure 2a, in which a red color indicates concordant upregulation of the 14q32.31 miRNAs, whereas a blue color indicates their downregulation. Upon analysis of the sample type within each group, we found a significantly higher number of normal samples in the high group and, conversely, a higher number of metastatic cases in the low group (P less than 0.001, Figure 2b). Lower 14q32.31miRNAs levels correlated significantly with a higher incidence of metastatic events, and a similar trend was observed for lymph node invasion (Figure 2c) and Gleason score (Supplementary Figure 2A). Furthermore, samples with low 14q32.31miRNAs expression had significantly higher PSA levels (Supplementary Figure 2B). We analyzed the expression of 14q32.31 miRNAs in a second data set generated from 139 human prostate adenocarcinoma tumors in the Cancer Genome Atlas project. These data are available at http://cancergenome.nih.gov/. The data set in miRNASeq consisted of seven miRNAs from the 14q32.31 cluster: miR-154, miR-376a, miR-376c, miR-377, miR-381, miR-487b and miR-495. Given the low expression of miR-376a (less than 2 reads per million miRNA mapped, r.p.m., for all samples), it was excluded from further analysis. As shown in Figure 2d, the remaining six miRNAs were expressed together and tightly correlated across the set. Figure 2e shows that samples with a low expression of these miRNAs were significantly enriched in N1 tumors (indicating nodal involvement). Information regarding metastasis was not available. Finally, Figure 2f shows the downregulated expression of miR-376c, miR-381 and miR-377 in tumors with nodal involvement versus those without. miRNAs 487b and 495 have a similar trend but were not significant (data not shown). The data sets by Taylor *et al.* and the Cancer Genome Atlas project together describe a consistent picture of PCa invasiveness and metastatic potential associated with low 14q32.31 miRNA levels.

14q32.31 miRNAs regulate cellular behaviors key to tumorigenicity

A myriad of studies have revealed deregulated miRNA levels in cancer, but whether such alterations directly cause tumorigenesis or simply result from changes in cellular phenotype remains unclear.[37–39] Thus, we singularly overexpressed 14q32.31 miRNAs to analyze their effect on cell behaviors important to carcinogenesis, namely, proliferation, apoptosis, migration and invasion. To study the effect of 14q32.31 miRNAs on cell cycle progression, we used flow cytometry to quantify the number of cells in each phase of the cell cycle through a BrdU and propidium iodide assay. The assay was carried out at 48 and 72 h post transfection in both PC3 and DU145 cells. Figure 3a depicts the dot blots of those miRNAs, which significantly decreased the number of cells in S phase of the cell cycle, accompanied by an increase in G1 cells. MiR-495 and miR-654-3p inhibited proliferation in both PC3 and DU145 cells at 48 h post transfection, whereas miR-376a had the same effect only in DU145 cells. The latter result suggests that miR-376a targets a cell cycle protein expressed in DU145 cells and not in the PC3 cell line. In contrast, miR-154, miR-377 and miR-485-3p impeded cellular proliferation in PC3 cells alone at 72 h post transfection. These miRNAs possibly target PC3-specific proteins important for cell cycle progression only in an indirect manner. We also used flow cytometry to quantify the numbers of live, apoptotic and necrotic cells at 72 h post transfection via a fluorescein diacetate (fluorescein DA) and propidium iodide (PI) assay.[40] MiR-299-5p and miR-654-3p induced apoptosis in DU145 cells alone (Figure 3b) as a result of either differential expression of apoptosis-related target proteins in DU145 and PC3 cells or a greater resistance to apoptosis in the PC3 cell line. Note that 14q32.31 miRNAs not shown in Figure 3a and b had no effect on proliferation and apoptosis (data not shown).

Next, we screened 14q32.31 miRNAs for possible inhibitory effects on cellular migration and invasion and graphed the results in Figures 4a and b. MiR-485-3p and miR-654-3p blocked migration and invasion in both PC3 and DU145 cells. MiR-377 impeded cell migration in both cell lines. MiR-376c and miR-299-5p inhibited migration in PC3 and DU145 cells, respectively, whereas miR-376a blocked migration and invasion in DU145 cells.

MiR-377 and miR-485-3p induce an epithelial phenotype in PC3 cells

Re-expression of miR-377 and miR-485-3p in the cell line PC3 caused the mesenchyme-like cells to retract and assume a more epithelial phenotype (Figure 5a). To support our observation, we studied the protein expression of epithelial markers ZO-1 and E Cadherin and the mesenchymal marker Ets-1 in PC3 cells transfected with a scrambled sequence or premiR-377/premiR-485-3p. The western blot images in Figure 5b demonstrate a marked increase in ZO-1 expression in cells expressing miR-377 and miR-485-3p. E cadherin expression increased significantly but to a lesser extent in miR-377-expressing cells. Ets-1 levels decreased upon expression of both miRNAs.

More importantly, we sought to determine whether the levels of miR-377 and miR-485-3p correlated with epithelial and mesenchymal markers in human prostate specimens from the Taylor *et al.* dataset. As these data are limited to the transcriptional level (excluding translational interactions), we focused on a transcriptional pattern characterizing epithelial–mesenchymal

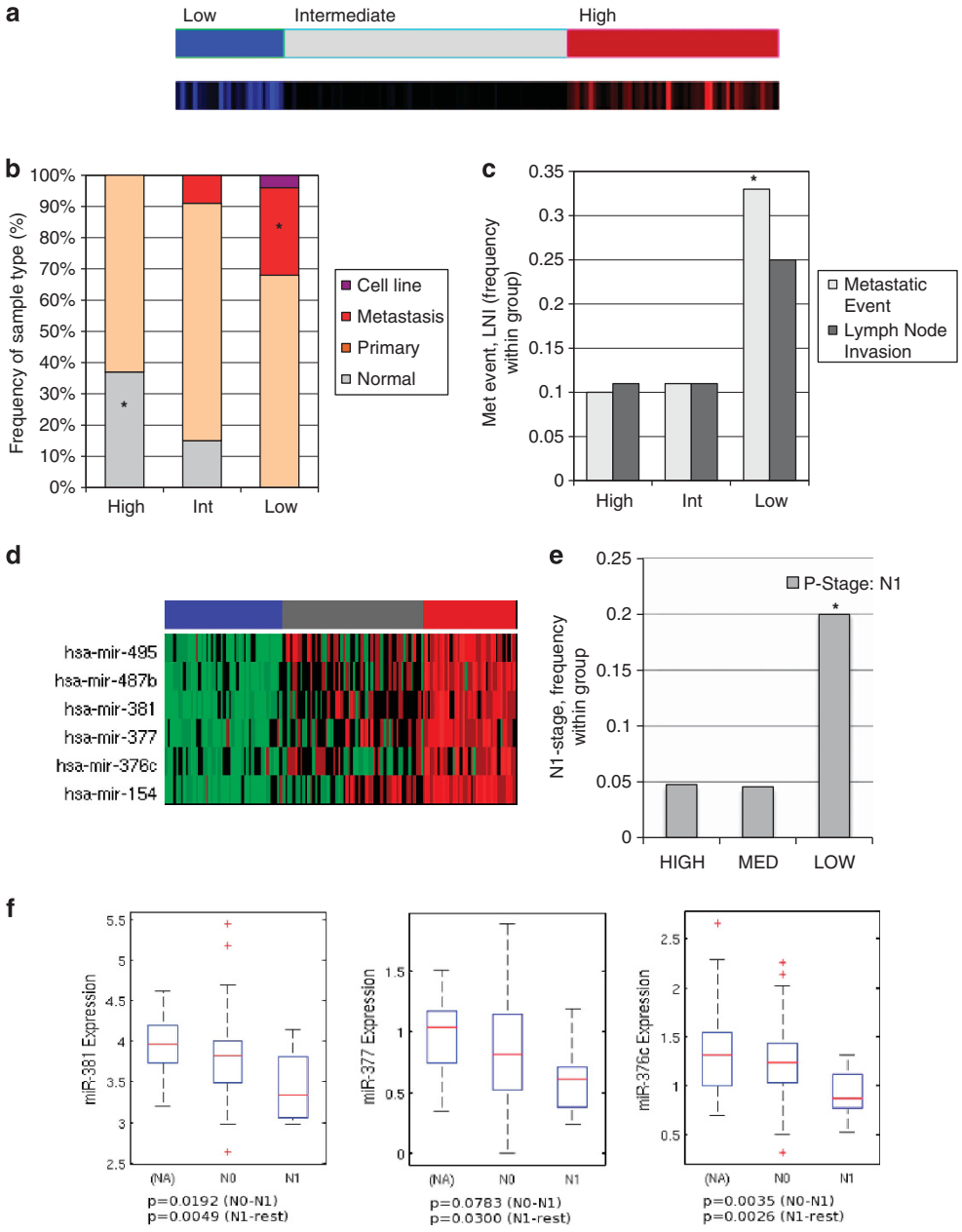

Figure 2. 14q32.31 miRNA cluster expression in clinical specimens. (**a**–**e**) The ten 14q32.31 miRNAs (154, 299-5p, 376a, 376c, 377, 381, 485-3p, 487b, 495 and 654-3p) included in the Taylor *et al.* data set (GSE21032) were combined into one miRNA-expression signature, and their concordant expression was evaluated using GSEA. (**a**) Heatmap showing 140 prostate samples clustered by the resulting signature scores, yielding three groups with high (red), intermediate, and low (blue) concordant expressions of the miRNAs. (**b**) Distribution of the sample type (cell line, metastasis, primary and normal) within high-, intermediate- and low-expression groups. A low expression of the miRNA-cluster is associated with metastases in prostate cancer, whereas a high expression of the miR-cluster is associated with normal samples (*$P < 1.0E-04$, Fischer Exact Test). (**c**) Frequency of metastatic events and lymph node invasion (LNI) within the three groups (*$P < 0.05$, Fischer Exact Test). (**d**) Clustering of log (data + 1)-transformed miRNA expression (reads per million mapped) from 139 tumors in the TCGA prostate cancer set. Of the 7 miRNAs belonging to the cluster, 6 are shown (one was sorted out due to low reads < 2 r.p.m). The miRNAs are clearly co-expressed in the set. (**e**) The group with low expression of the miRNAs showed significant enrichment in tumors with P stage N1 (nodal involvement, *$P < 0.01$, Fischer Exact Test). Remaining tumors were stage N0 or not annotated. (**f**) Levels of individual miRNAs differ significantly between N1 and N0 tumors (*t*-test, *P*-values indicated), with lower levels in N1 invasive tumors.

Figure 3. The subset of 14q32.31 miRNAs induce cell cycle arrest and apoptosis in PC3 and DU145 cells. Ten miRNAs of the 14q32.31 cluster (miR-154, miR-299-5p, miR-376a, miR-376c, miR-377, miR-381, miR-485-3p, miR-487b, miR-495 and miR-654-3p) were overexpressed in PC3 and DU145 cells and analyzed for effects on cell cycle (at 48 and 72 h) and apoptosis (72 h). (**a**) Effects on cell cycle progression are shown for those miRNAs that significantly reduced ($P < 0.05$ by student's *t*-test; $n = 3$) cells in S-phase (y-axis; BrdU) as compared with control cells transfected with a scrambled sequence. The x-axes denote DNA content by fluorescence of the DNA dye (PI). Images and cell percentages of one sample experiment are given. (**b**) Quantitative analysis of cell viability and death by flow cytometric measurement of cellular fluorescence after staining with fluorescein diacetate (FDA, x-axis) and propidium iodide (PI). The percentages indicate necrotic (N, top left), apoptotic (A, bottom left) and live cells (L, bottom right). Images based on one experiment are shown for those miRNAs that induced apoptosis in a significant manner based on three independent trials ($P < 0.05$, Student's *t*-test).

transition, derived by Sarrio *et al.*[41] after experimentally inducing and observing the transition in MCF10A cell lines (density array). In particular, this study published a list of genes that were upregulated under EMT (EMT-UP) and a list of genes that were downregulated under EMT (EMT-DWN). Using both lists as expression signatures, one obtains a cross-check measure of the EMT process: the presence

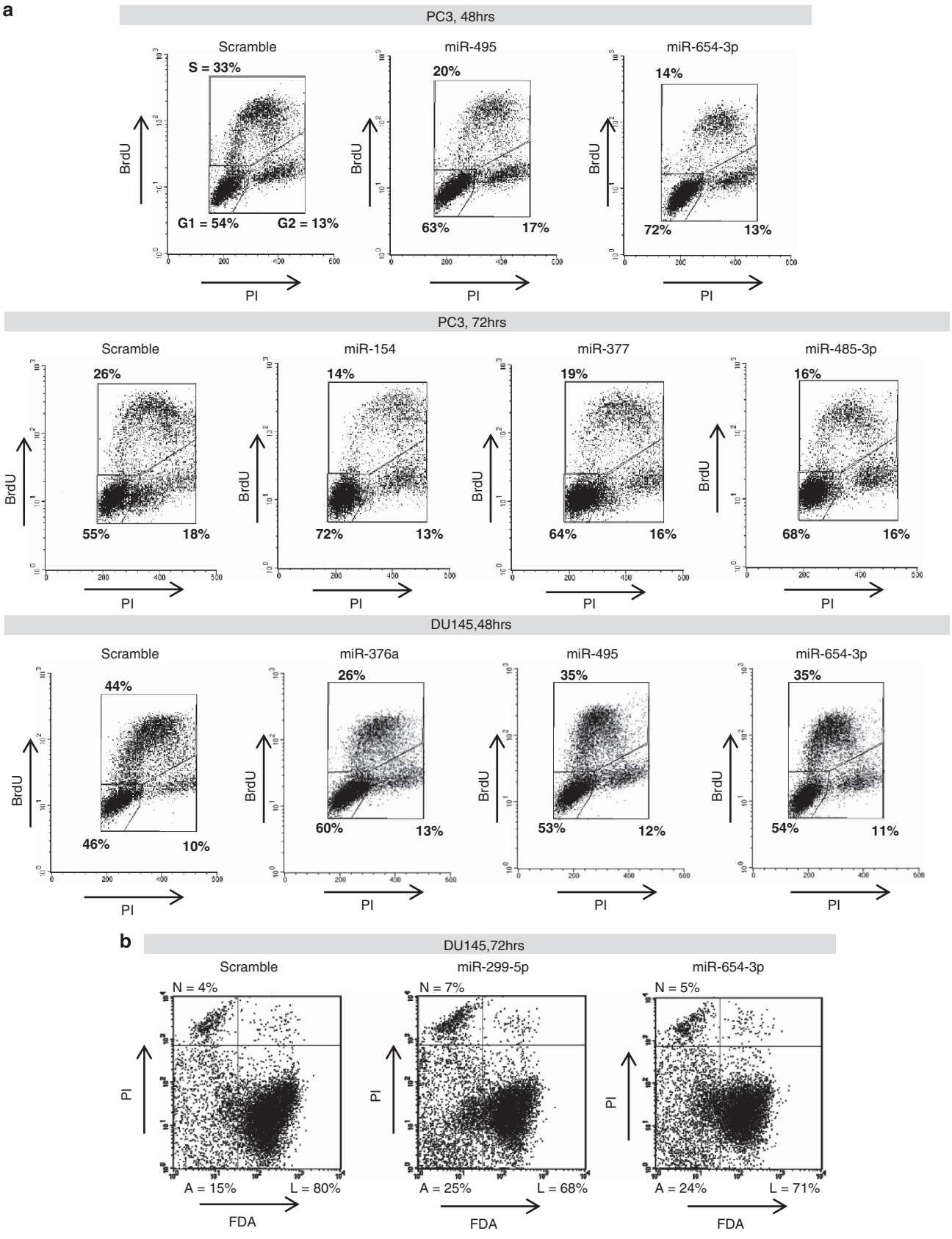

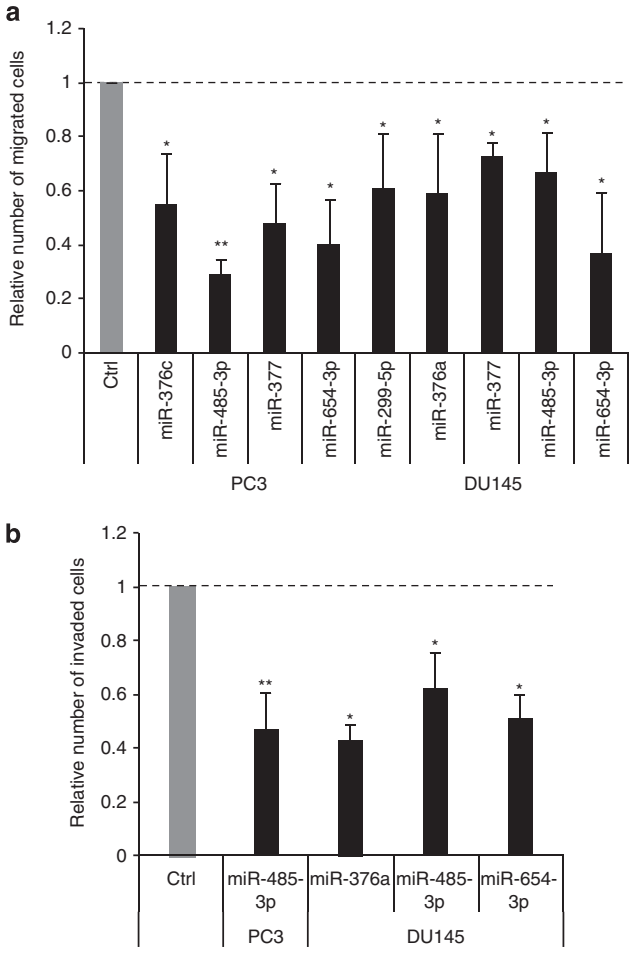

Figure 4. 14q32.31 miRNAs impede cellular migration and invasion. Ten miRNAs of the 14q32.31 cluster (miR-154, miR-299-5p, miR-376a, miR-376c, miR-377, miR-381, miR-485-3p, miR-487b, miR-495 and miR-654-3p) were overexpressed in PC3 and DU145 cells and analyzed for their ability to migrate (**a**) and invade (**b**) as compared with control cells (Ctrl) transfected with a scrambled sequence. In both (**a**) and (**b**), miRNAs with the capacity to inhibit cellular migration and invasion are shown. Results are reported as fold changes with control cells set to 1. Error bars represent the standard deviation of at least three independent experiments. $*P<0.05$; $**P<0.01$ by Student's *t*-test.

of EMT should result in the EMT-UP signature to be highly expressed and the EMT-DWN signature to be underexpressed, whereas the reverse pattern should indicate the absence of the EMT process. We calculated the signature scores for both signatures using gene set enrichment analysis on the mRNA data and compared the resulting scores with the expression levels of miR-377 and miR-485-3p. Heatmaps showing both the EMT signature scores (lower two bars, Figure 5c) and the miRNA expression levels (middle bar) sorted by sample type (top bar) indicate an association of miR-377 loss (blue colors) with an EMT process (EMT-UP red colors, EMT-DWN blue colors) concentrated in metastatic samples. Consistently, the EMT process was absent in most normal samples, along with increased expression of miR-377. MiR-485-3p expression, although itself more variable (compare color intensity of the middle bar), was less correlated with the EMT signature scores. We calculated the Pearson correlation coefficient between signature scores and miRNA expression for both miRNAs and found a significant correlation between miR-377 expression and both signatures (as expected in reverse directions, *P* less than 1.0e-05), whereas the data for miR-485-3p showed the same trend but did not produce significant correlations (Figure 5d). Together, these data suggest that the loss of miR-377 expression coincides with the gain of an epithelial–mesenchymal transition expression pattern and vice versa. For miR-485-3p, a weak trend was observed.

miR-377 targets FZD4 in human prostate cancer

We next sought to identify a target of miR-377 that could be responsible for its anti-tumorigenic effect in PC3 cells. We used TargetScan6.2 software to search for putative targets implicated as oncogenes in the literature. TargetScan revealed that frizzled 4 (FZD4) mRNA possesses one conserved and two poorly conserved putative miR-377 target sites in its 3′-UTR. FZD4 has been implicated as a mediator of epithelial-to-mesenchymal transition in human (PCa) cells.[42]

We correlated the expression of miR-377 to FZD4 mRNA using the clinical data available in the data set by Taylor *et al.*[35] and found a highly significant ($P=0.003$) negative correlation (Figure 6a). Next, to support the notion of FZD4 as a putative oncogene in our context, we analyzed the expression of FZD4 mRNA in normal, tumor and metastatic samples of the data set and found a significant upregulated trend across the groups (Figure 6b).

We analyzed the mRNA and protein expression of FZD4 in PC3 cells transfected with a scrambled sequence or premiR-377. PremiR-377 decreased the mRNA levels of FZD4 by about 50% (Figure 6c), accompanied by a reduction in protein levels as evidenced by western blotting (Figure 6d). To confirm FZD4 as a direct miR-377 target, we cloned part of its 3′-UTR sequence downstream to a luciferase reporter gene and transfected the resulting vector in the presence of premiR-377 or a scrambled sequence as control. The histogram in Figure 6e shows an approximate 40% reduction in luciferase activity after miR-377 overexpression compared with the control (set to 100%).

Finally, we used RNA interference to verify the cancer-promoting role of FZD4 in PC3 cells. Figure 6f illustrates the significant anti-migratory and anti-invasive effects of FZD4 knockdown in these cells.

DISCUSSION

In this study, we implicate the large miRNA cluster at 14q32.31 in human PCa for the first time. The expression of miRNAs in this cluster exhibits a remarkable downregulation in PCa metastatic cell lines. The trend resurfaces in samples of human PCa, whereby expression of the cluster diminishes in primary tumors and more so in metastatic cases. Prostate tissue samples with a low expression of the cluster have significantly higher incidences of metastatic events as well as higher levels of PSA, a marker linked to tumor stage and prognosis.[43] Moreover, the majority of cases of normal prostate tissue have high levels of the cluster. These data suggest that, although 14q32.31 miRNAs may contribute to the initial phase of tumor formation, they participate to a greater extent in its progression to a more aggressive state. Besides 14q32.31 miRNAs, other miRNAs have been associated to cytoskeleton remodeling and migration in epithelial cells.[44–46]

After confirming the downregulation of 14q32.31 miRNAs in a cohort of PCa patients, we sought to identify the underlying silencing mechanism. Previous reports have identified genomic loss in this area[47] as well as epigenetic alterations that silence the cluster.[24] We hypothesized that deletions in the genomic region harboring these miRNAs and/or epigenetic abnormalities could lead to their deregulation. In patient samples, we did not observe any differences in DNA copy number corresponding to the miRNAs of interest, thus leading to the conclusion that the former mechanism does not regulate the transcription of 14q32.31 miRNAs. In contrast, dual treatment of PCa cell lines

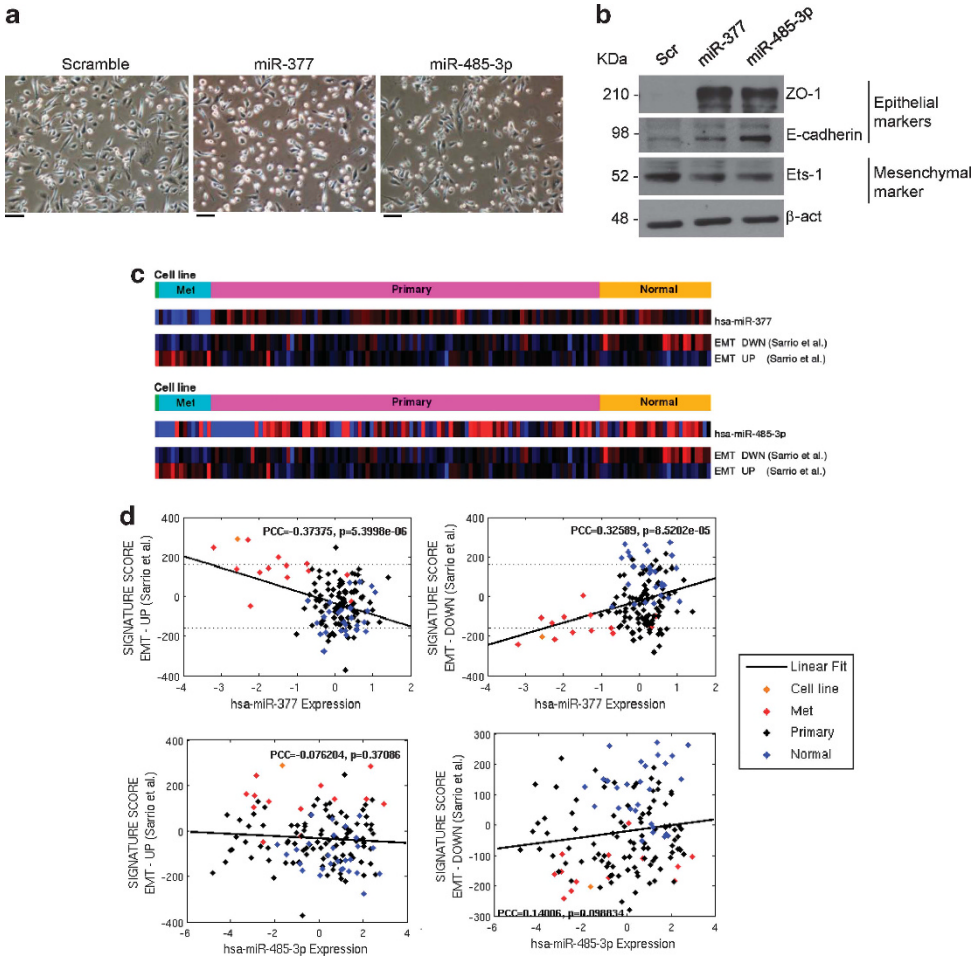

Figure 5. miR-377 and miR-485-3p re-expressions provoke an epithelial phenotype in PC3 cells. (**a**) Phase-contrast microscopic images of PC3 cells transfected with either a scrambled sequence, premiR-377 or premiR-485-3p. Both miRNAs 377 and 485-3p cause cells to retract, thus adopting a more rounded and a less spindle-shaped phenotype. Black bar length is 83 μm. (**b**) Western blot images showing an increase in epithelial (ZO-1, E-Cadherin) protein expression and a concomitant decrease in mesenchymal (Ets-1) protein expression in control and premiR-377/485-3p-expressing cells. (**c**) Heatmap displaying miR-377 (upper map) and miR-485-3p (lower map) expression with the expression of a transcriptional signature pair characterizing epithelial–mesenchymal transition (EMT-UP, EMT-DWN). In both cases, samples were sorted by type as indicated in top bars. Note that, although middle bars represent expression values of the miRNAs (true red corresponding to at least twofold expression over mean and true blue at least twofold expression under mean), the lower bars represent significant signature scores (true red and true blue corresponding to significant high scores and low scores, respectively, with p less than 1.0e-05). Notably, the loss of expression of miR-377 coincides with gain of the EMT-UP and loss of the EMT-DWN signature in metastatic samples, producing a consistent transcriptional pattern indicating EMT in these samples. (**d**) Quantification of the correlation between miRNA expression (miR-377, miR-485-3p) and signature scores as calculated by GSEA (details see Methods). Pearson correlation coefficients and *P*-values are indicated in each box. Samples are color-coded by type.

with inhibitors of DNA methyltransferase enzymes as well as histone deacetylases affected a surge in miRNA levels, thus suggesting epigenetic control over their expression. However, such increased expression exhibited certain inconsistencies. For example, miR-154 did not respond to any treatment in either DU145 or PC3 cells. MiR-654-3p increased in expression by hundreds of folds after dual-drug treatment in DU145 cells, while showing no change in the PC3 cell line. Clearly, other means of transcriptional and/or posttranscriptional control cooperate with epigenetic mechanisms to regulate the expression of 14q32.31 miRNAs in the human prostate.

We attempted to understand whether the deregulated expression of 14q32.31 miRNAs in PCa occurred as a consequence of cellular transformation or as a necessary component to its realization. Thus, we re-expressed 10 miRNAs of the cluster in PCa cell lines to see what role they might have in malignant cell behaviors. Six miRNAs (miR-154, miR-377, miR-376a, miR-485-3p, miR-495 and miR-654-3p) altered cell cycle progression in DU145 and/or PC3 cells and in all cases affected a decrease in proliferative S phase cells accompanied by an increase in G1 cells. Two miRNAs (miR-299-5p and miR-654-3p) caused cells to undergo apoptosis in DU145 cells. Six miRNAs (miR-376a, miR-376c, miR-299-5p, miR-377, miR-485-3p and miR-654-3p) reduced cell migration and/or invasion in at least one cell line. Of the 10 miRNAs analyzed here, 8 had an anti-tumorigenic effect on one or more hallmarks of cancer cell behavior, thus supporting previous hypotheses that miRNAs in this cluster function as tumor-suppressor genes.[24] Importantly, miR-485-3p and miR-377 sustained a mesenchymal-to-epithelial transition in the highly aggressive cell line PC3. Further analysis in a large patient cohort revealed a significant correlation between miR-377 levels and EMT genes. To further go into the molecular mechanism, we identified frizzled 4 (FZD4) as an miR-377 target. We conducted a 3′-UTR lucifease assay and observed that the luciferase activity was decreased after co-transfection of miR-377 with a 3′-UTR vector containing the

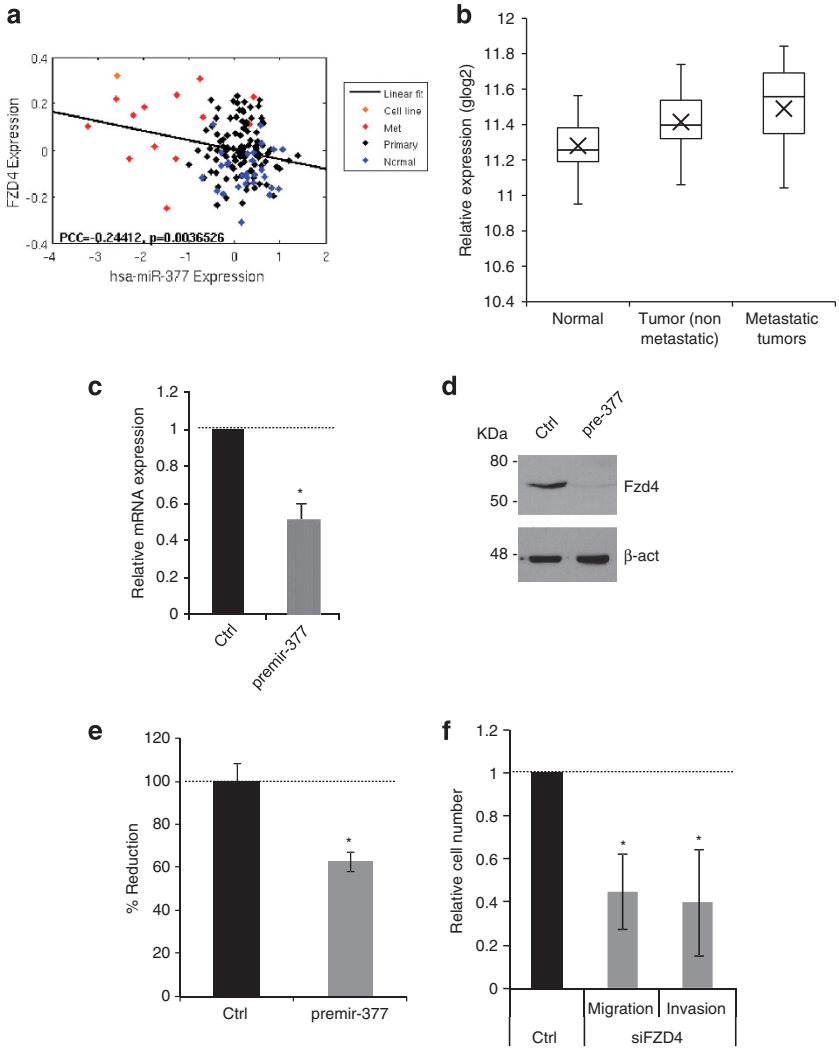

Figure 6. FZD4 is an miR-377 direct target. (**a**) miR-377 expression correlates negatively with target mRNA expression in metastatic PCa samples present in the clinical data available in the data set by Taylor *et al.*[35] Bottom left: the Pearson correlation coefficient (PCC) and associated *P*-value. (**b**) Box and whisper plots of FZD4 mRNA levels in normal, non metastatic tumors and metastatic samples of the same data set show a significant upregulated trend across the groups ($P<0.0001$, ANOVA). (**c**) Relative mRNA levels of FZD4 in control (Ctrl) and miR-377-expressing cells at 48 h after transfection as determined by RT-qPCR. **P*-value <0.05 as determined by Student's *t*-test. (**d**) FZD4 protein levels 48 h after transfection as determined by western blotting. β-actin expression was used as a loading control. (**e**) Insertion of a fragment from FZD4 3′-UTR in a luciferase reporter gene construct leads to decreased luciferase activity in the presence of miR-377 in HEK-293E cells 24 h after co-transfection. Histogram shows the percentage of reduction in the luciferase activity of miR-377 compared with scramble-control-transfected cells set to 100%. Data are shown as the average ± S.D. from three independent assays. **P*-value <0.05 by Student's *t*-test. (**f**) FZD4 was silenced by an siRNA in PC3 cells. Silenced cells were analyzed for their ability to migrate and invade as compared with control cells (Ctrl) transfected with a scrambled sequence. Results are reported as fold changes with control cells set to 1. Error bars represent the standard deviation of at least three independent experiments. **P*-value <0.05, by Student's *t*-test.

FZD4 target sequence. FZD4 protein expression was also significantly downregulated in miR-377-transfected cells, indicating that FZD4 is a direct target of miR-377. FZD4 knockdown in PC-3 cells, mimicking overexpression of miR-377, resulted in a significant anti-migratory and anti-invasive effect, in agreement with previous data shown in bladder cancer.[48] Analyzing the clinical data available in the data set by Taylor *et al.*, we found a highly significant ($P=0.003$) negative correlation between FZD4 and miR-377 expression patterns. Furthermore, to support the notion of FZD4 as a putative oncogene in PCa, we analyzed the expression of FZD4 mRNA in normal, tumor and metastatic samples of the data set and found a significant upregulated trend across the groups.

In conclusion, our study suggests that miRNAs mapped to the 14q32.31 have an important role as tumor-suppressive miRNAs inhibiting cell proliferation, invasion and migration in metastatic PCa. In addition, the miR-377 target, FZD4, contributes significantly to the epithelial-to-mesenchymal transition observed in metastaic PCa cell lines. More importantly, our study suggests the potential of miR-377 as a clinically useful marker of malignancy in PCa.

MATERIALS AND METHODS

Cell lines and treatment with 5-aza-2′-deoxycytidine and Trichostatin A

PC3 and DU145 were purchased from the American Type Cell Collection (Manassas, VA, USA) and cultured as recommended by their vendor. Cells were treated for 72 h with 5 μM of 5-aza-2′-deoxycytidine (Sigma, St Louis, MO, USA) refreshed daily. The same protocol was followed for Trichostatin A (Sigma) treatment with H_2O instead of AZA. An amount of 500 nM of trichostatin A was added for the last 16 h.

RNA extraction, reverse transcription and quantitative PCR of mRNA and mature miRNA sequences

For both mRNA and miRNA quantification, total RNA was extracted using the mirVanamiRNA isolation kit (Ambion, AM1561, Life Technologies, Grand Island, NY, USA). For miRNA analysis, TaqManmiRNA assays (Applied Biosystems, Life Technologies, Grand Island, NY, USA) were used to measure expression levels by a multiplex RT reaction. The 20 μL RT reaction contained the following reagents available in the TaqmanmiRNA reverse transcription kit (Applied Biosystems): 0.4 μl dNTP, 4 μl reverse transcriptase, 2 μl 10X RT buffer, 0.25 μl RNase inhibitor, 20 ng RNA and 4 μl 5X primer pool. The primer pool consisted of the Taqman RT primers each diluted 1:4 from 250 nM to 62.5 nM. The 16 μl qPCR reaction contained the 2XTaqmanqPCR master mix, 0.4 μl of Taqman probe and 3 μl of fivefold diluted cDNA. qPCR was carried out on the ABI 7500 instrument (Applied Biosystems). The geometric mean of miR-191 and miR-103 was used as a qPCR normalizer.[49,50] For mRNA analysis, total RNA was retro-transcribed with the InPromII Reverse Transcription System (Promega, Madison, WI, USA, A3800) according to the manufacturer's recommendations. The 20 μl qPCR reaction consisted of 2X Platinum SYBR Green qPCRSuperMix UDG (Invitrogen, Life Technologies, Grand Island, NY, USA, 11733-046), 10 ng cDNA and 0.4 μM of forward and reverse primers. The geometric mean of beta-actin (forward: 5′-CTGGCACCACACCTTCTACAATG-3′; reverse: 5′-tagca cagcctggatagcaac-3′) and B2M (forward: 5′-catccatccgacattgaagt-3′; reverse: 5′-gaaagaccagtccttgctga-3′) was used as a normalizer. The primer sequences used for FZD4 are: 5′-ggtgcccttacctcacaaaacc-3′ (forward) and 5′-gccagcatcatagccacacttg-3′ (reverse). The specificity of the PCR reaction was monitored by a melt–curve protocol. For both mRNA and miRNA quantification, data were imported into qBase^{PLUS} (Biogazelle, Zwijnaarde, Belgium) for analysis of reference gene quality control and relative quantification.

Re-expression of miRNA sequences in cell lines

PC3 and DU145 cells were transfected with either a scrambled negative control sequence (Ctrl) or the following premiRNA sequences (Ambion): 154, 299-5p, 376a, 376c, 377, 381, 485-3p, 487b, 495 and 654-3p. Forward transfections with the lipofectamine RNAiMax Reagent (Invitrogen 13778-150) were carried out according to the manufacturer's protocol with 30 nM of premiRNA oligonucleotides.

Cellular proliferation, apoptosis, migration and invasion assays

For proliferation assays, cells were 4 h pulse-labeled with 10 μM of the BrdU analog, EdU (5-ethynyl-2′-deoxyuridine) and then processed with the Click-iT EdU Alexa Fluor 488 Flow Cytometry Assay Kit (Invitrogen C10425). Proliferating (EdU positive) cells were analyzed and quantified with a BD FACSCalibur Flow Cytometer (Becton Dickinson, Franklin Lakes, NJ, USA). For proliferation assays at 72 h, cells were split at 48 h post transfection, allowed to recover for 24 h and then pulse-labeled with EdU. This was necessary to prevent G1 arrest due to confluency at the 72 h time point.

Quantitative analysis of cell viability and death was performed by flow cytometric measurement of cellular fluorescence after staining with fluorescein diacetate and propidium iodide.[40] Cells were collected at 72 h post transfection and stained for 5′ with propidium iodide and fluorescein DA at a final concentration of 4 μg/ml and 100 mM, respectively. For both migration and invasion assays, cells were transfected with either a scrambled or a pre-miRNA sequence as outlined above. At 48 h post transfection, approximately 40 000 cells (migration) or 80 000 cells (invasion) were resuspended in FBS-free medium and seeded in a BD BioCoat control cell culture insert (BD Biosciences, San Jose, CA, USA; Catalog No. 354578) or a BD BioCoatmatrigel invasion chamber (BD Bioscience, Catalog No. 354480) for migration and invasion analysis, respectively. Note that migration/invasion inserts were placed in wells containing medium with 10% FBS so as to create a chemoattractive gradient. Twenty-four hours later, migrated/invaded cells were fixed, stained with crystal violet and counted using phase-contrast microscopy.

Western blotting

Total cell extracts were resolved on SDS polyacrylamide gels and blotted onto the Hybond PVDF membrane (GE Healthcare, Milano, Italia, RPN303F). Membranes were blocked with PBST 5% non-fat dry milk, incubated with primary antibodies for 2 h at room temperature, washed and hybridized with peroxidase-conjugated secondary antibodies for 1 h (Biorad goat anti-rabbit 166-2408EDU or goat anti-mouse 170–6520, Biorad, Hercules, CA, USA. Detection was performed with the ECL chemiluminescence kit (Perkin Elmer, Waltham, MA, USA; NEL105001EA). The antibodies used were as follows: anti-ZO1 (Invitrogen 40–2200, 1/1000 dilution), anti-β-actin (Sigma A5441, 1/5000 dilution), anti E cadherin (Cell Signaling, Danvers, MA, USA; 5296), anti ETS-1 (Santa Cruz, Dallas, TX, USA; sc-350) and anti-FZD4 (Abcam, Cambridge, UK; ab77724 1/1000).

Luc assay and constructs

A fragment of FZD4 constituting 460 bp of FZD4's 3′UTR sequence containing the miR-377 target site were amplified by PCR from human genomic DNA using the following primer pair: 3′UTR-FZD4-F 5′-GGCCTCT AGATCTGTGGTGCGCTGTCTGCTGT-3′ and 3′UTR-FZD4-R 5′-GGCCTCTAGA AAACTTAACATTTCAGCTCTTC-3′. PCR fragments were restricted and ligated to a compatible Xbal-linearized pGL3Control vector (Promega). A total of 2 × 10e5 HEK 293E cells were seeded in 12-well dishes 24 h before transfection. Amounts of 100 ng of pGL3Control vector, 12pmol of pre-miR or scrambled control sequence (Ambion) and 10 ng of Renilla luciferase pRL-CMV vector (Promega) were co-transfected using Lipofectamine 2000 (Invitrogen). Luciferase activities of cellular extracts were measured 24 h after transfection using a Dual Luciferase Reporter Assay System (Promega). Light emission was measured over 10 s using a Lumat LB9507 luminometer (EG&G Berthold, Bad Wildbad, Germany). Efficiency of transfection was normalized using the Renilla luciferase activity.

Bioinformatics

MiR-377 target site on the FZD4 3′-UTR was predicted by TargetScan 5.1 software available at www.targetscan.org.

ABBREVIATIONS

miRNA, MicroRNA; PCa, Prostate cancer; PrEC, normal prostatic epithelial cells; PSA, prostate-specific antigen.

CONFLICT OF INTEREST

The authors declare no conflict of interest.

ACKNOWLEDGEMENTS

This work has been mainly supported by AIRC grant (2013IG 13387) to EC and partially supported by AIRC (2011-IG11955) and Ministry of Education and Science of the Russian Federation (11.G34.31.0069) to GM. Research described in this article was also supported in part by Min. Salute (ric. Oncologica26/07), 'IstitutoDermopatico-dell'Immacolata' (RF06 c.73, RF07 c.57, RF08 c.15, RF07 c.57) to GM.

REFERENCES

1 Ferlay J, Shin HR, Bray F, Forman D, Mathers C, Parkin DM. *GLOBOCAN 2008 v1.2, Cancer Incidence and Mortality Worldwide: IARC CancerBase No. 10 [Internet]*. International Agency for Research on Cancer: Lyon, France, 2010, Available from: http://globocan.iarc.fr. Accessed May 2011.
2 Gandellini P, Profumo V, Casamichele A, Fenderico N, Borrelli S, Petrovich G *et al.* miR-205 regulates basement membrane deposition in human prostate: implications for cancer development. *Cell Death Differ* 2012; **19**: 1750–1760.
3 Hudson RS, Yi M, Esposito D, Glynn SA, Starks AM, Yang Y *et al.* MicroRNA-106b-25 cluster expression is associated with early disease recurrence and targets caspase-7 and focal adhesion in human prostate cancer. *Oncogene* 2012; **32**: 4139–4147.
4 Boll K, Reiche K, Kasack K, Mörbt N, Kretzschmar AK, Tomm JM *et al.* MiR-130a, miR-203 and miR-205 jointly repress key oncogenic pathways and are down-regulated in prostate carcinoma. *Oncogene* 2013; **32**: 277–285.
5 Martens-Uzunova ES, Jalava SE, Dits NF, van Leenders GJ, Møller S, Trapman J *et al.* Diagnostic and prognostic signatures from the small non-coding RNA transcriptome in prostate cancer. *Oncogene* 2012; **31**: 978–991.
6 Musumeci M, Coppola V, Addario A, Patrizii M, Maugeri-Saccà M, Memeo L *et al.* Control of tumor and microenvironment cross-talk by miR-15a and miR-16 in prostate cancer. *Oncogene* 2011; **30**: 4231–4242.
7 Takayama K, Tsutsumi S, Katayama S, Okayama T, Horie-Inoue K, Ikeda K *et al.* Integration of cap analysis of gene expression and chromatin immunoprecipitation analysis on array reveals genome-wide androgen receptor signaling in prostate cancer cells. *Oncogene* 2011; **30**: 619–630.
8 Hassan O, Ahmad A, Sethi S, Sarkar FH. Recent updates on the role of microRNAs in prostate cancer. *J Hematol Oncol* 2012; **5**: 9.

9 Nair VS, Maeda LS, Ioannidis JP. Clinical outcome prediction by microRNAs in human cancer: a systematic review. *J Natl Cancer Inst* 2012; **104**: 528–540.
10 Antonov AV, Knight RA, Melino G, Barlev NA, Tsvetkov PO. MIRUMIR: an online tool to test microRNAs as biomarkers to predict survival in cancer using multiple clinical data sets. *Cell Death Differ* 2013; **20**: 367.
11 Viticchiè G, Lena AM, Cianfarani F, Odorisio T, Annicchiarico-Petruzzelli M, Melino G *et al.* MicroRNA-203 contributes to skin re-epithelialization. *Cell Death Dis* 2012; **3**: e435.
12 Tucci P, Agostini M, Grespi F, Markert EK, Terrinoni A, Vousden KH *et al.* Loss of p63 and its microRNA-205 target results in enhanced cell migration and metastasis in prostate cancer. *Proc Natl Acad Sci USA* 2012; **109**: 15312–15317.
13 Aberdam D, Candi E, Knight RA, Melino G. miRNAs, 'stemness' and skin. *Trends Biochem Sci* 2008; **33**: 583–591.
14 Lena AM, Shalom-Feuerstein R, Rivetti di Val Cervo P, Aberdam D, Knight RA, Melino G *et al.* miR-203 represses 'stemness' by repressing DeltaNp63. *Cell Death Differ* 2008; **15**: 1187–1195.
15 Seitz H, Royo H, Bortolin ML, Lin SP, Ferguson-Smith AC, Cavaillé J. A large imprinted microRNA gene cluster at the mouse Dlk1-Gtl2 domain. *Genome Res* 2004; **14**: 1741–1748.
16 Olive V, Jiang I, He L. mir-17-92, a cluster of miRNAs in the midst of the cancer network. *Int J Biochem Cell Biol* 2010; **42**: 1348–1354.
17 Aqeilan RI, Calin GA, Croce CM. miR-15a and miR-16-1 in cancer: discovery, function and future perspectives. *Cell Death Differ* 2010; **17**: 215–220.
18 da Rocha ST, Edwards CA, Ito M, Ogata T, Ferguson-Smith AC. Genomic imprinting at the mammalian Dlk1-Dio3 domain. *Trends Genet* 2008; **24**: 306–316.
19 Zehavi L, Avraham R, Barzilai A, Bar-Ilan D, Navon R, Sidi Y *et al.* Silencing of a large micro-RNA cluster on human chromosome 14q32 in melanoma: biological effects of mir-376a and mir-376c on insulin growth factor 1 receptor. *Mol Cancer* 2012; **11**: 44.
20 Costa FF, Bischof JM, Vanin EF, Lulla RR, Wang M, Sredni ST *et al.* Identification of microRNAs as potential prognostic markers in ependymoma. *PLoS One* 2011; **6**: e25114.
21 Thayanithy V, Sarver AL, Kartha RV, Li L, Angstadt AY, Breen M *et al.* Perturbation of 14q32 miRNAs-cMYC gene network in osteosarcoma. *Bone* 2012; **50**: 171–181.
22 Gattolliat CH, Thomas L, Ciafrè SA, Meurice G, Le Teuff G, Job B *et al.* Expression of miR-487b and miR-410 encoded by 14q32.31 locus is a prognostic marker in neuroblastoma. *Br J Cancer* 2011; **105**: 1352–1361.
23 Haller F, von Heydebreck A, Zhang JD, Gunawan B, Langer C, Ramadori G *et al.* Localization- and mutation-dependent microRNA (miRNA) expressionsignatures in gastrointestinal stromal tumours (GISTs), with a cluster of co-expressed miRNAs located at 14q32.31. *J Pathol* 2010; **220**: 71–86.
24 Zhang L, Volinia S, Bonome T, Calin GA, Greshock J, Yang N *et al.* Genomic and epigenetic alterations deregulate microRNAexpression in human epithelial ovarian cancer. *Proc Natl Acad Sci USA* 2008; **105**: 7004–7009.
25 Devor EJ, DE Mik JN, Ramachandran S, Goodheart MJ, Leslie KK. Global dysregulation of the chromosome 14q32 imprinted region in uterine carcinosarcoma. *Exp Ther Med* 2012; **3**: 677–682.
26 Lavon I, Zrihan D, Granit A, Einstein O, Fainstein N, Cohen MA *et al.* Gliomas display a microRNA expression profile reminiscent of neural precursor cells. *NeuroOncol* 2010; **12**: 422–433.
27 Zhang H, Li Y, Huang Q, Ren X, Hu H, Sheng H *et al.* MiR-148a promotes apoptosis by targeting Bcl-2 in colorectal cancer. *Cell Death Differ* 2011; **18**: 1702–1710.
28 Afanasyeva EA, Mestdagh P, Kumps C, Vandesompele J, Ehemann V, Theissen J *et al.* MicroRNA miR-885-5p targets CDK2 and MCM5, activates p53 and inhibits proliferation and survival. *Cell Death Differ* 2011; **18**: 974–984.
29 Puisségur MP, Mazure NM, Bertero T, Pradelli L, Grosso S, Robbe-Sermesant K *et al.* miR-210 is overexpressed in late stages of lung cancer and mediates mitochondrial alterations associated with modulation of HIF-1 activity. *Cell Death Differ* 2011; **18**: 465–478.
30 Lin J, Teo S, Lam DH, Jeyaseelan K, Wang S. MicroRNA-10b pleiotropically regulates invasion, angiogenicity and apoptosis of tumor cells resembling mesenchymal subtype of glioblastomamultiforme. *Cell Death Dis* 2012; **3**: e398.
31 Kappelmann M, Kuphal S, Meister G, Vardimon L, Bosserhoff AK. MicroRNA miR-125b controls melanoma progression by direct regulation of c-Jun protein expression. *Oncogene* 2012; **32**: 2984–2991.
32 Couts KL, Anderson EM, Gross MM, Sullivan K, Ahn NG. Oncogenic B-Rafsignaling in melanoma cells controls a network of microRNAs with combinatorial functions. *Oncogene* 2013; **32**: 1959–1970.
33 Streicher KL, Zhu W, Lehmann KP, Georgantas RW, Morehouse CA, Brohawn P *et al.* A novel oncogenic role for the miRNA-506-514 cluster in initiating melanocyte transformation and promoting melanoma growth. *Oncogene* 2012; **31**: 1558–1570.
34 Formosa A, Lena AM, Markert EK, Cortelli S, Miano R, Mauriello A *et al.* DNA methylation silences miR-132 in prostate cancer. *Oncogene* 2012; **32**: 127–134.
35 Taylor BS, Schultz N, Hieronymus H, Gopalan A, Xiao Y, Carver BS *et al.* Integrative genomic profiling of human prostate cancer. *Cancer Cell* 2010; **18**: 11–22.
36 Kent WJ, Sugnet CW, Furey TS, Roskin KM, Pringle TH, Zahler AM *et al.* The human genome browser at UCSC. *Genome Res* 2002; **12**: 996–1006.
37 Cerami Ethan, Gao J, Dogrusoz U, Gross BE, Sumer SO, Aksoy BA *et al.* The cBio cancer genomics portal: an open platform for exploring multidimensional cancer genomics data. *Cancer Discov* 2012; **2**: 401.
38 Macfarlane LA, Murphy PR. MicroRNA: biogenesis, function and role in cancer. *Curr Genomics* 2010; **11**: 537–561.
39 Barlev NA, Sayan BS, Candi E, Okorokov AL. The microRNA and p53 families join forces against cancer. *Cell Death Differ* 2010; **17**: 373–375.
40 Bartkowiak D, Högner S, Baust H, Nothdurft W, Röttinger EM. Comparative analysis of apoptosis in HL60 detected by annexin-V and fluorescein-diacetate. *Cytometry* 1999; **37**: 191–196.
41 Sarrió D, Rodriguez-Pinilla SM, Hardisson D, Cano A, Moreno-Bueno G, Palacios J. Epithelial-mesenchymal transition in breast cancer relates to the basal-like phenotype. *Cancer Res* 2008; **68**: 989–997.
42 Gupta S, Iljin K, Sara H, Mpindi JP, Mirtti T, Vainio P *et al.* FZD4 as a mediator of ERG oncogene-induced WNT signaling and epithelial-to-mesenchymal transition in human prostate cancer cells. *Cancer Res* 2010; **70**: 6735–6745.
43 Kuriyama M, Obata K, Miyagawa Y, Nishikawa E, Koide T, Takeda A *et al.* Serum prostate-specific antigen values for the prediction of clinical stage and prognosis in patients with prostate cancer: an analysis of 749 cases. *Int J Urol* 1996; **3**: 462–467.
44 Amelio I, Lena AM, Viticchiè G, Shalom-Feuerstein R, Terrinoni A, Dinsdale D *et al.* miR-24 triggers epidermal differentiation by controlling actin adhesion and cell migration. *J Cell Biol* 2012; **199**: 347–363.
45 Jurmeister S, Baumann M, Balwierz A, Keklikoglou I, Ward A, Uhlmann S *et al.* MicroRNA-200c represses migration and invasion of breast cancer cells by targeting actin-regulatory proteins FHOD1 and PPM1F. *Mol Cell Biol* 2012; **32**: 633–651.
46 Yu J, Peng H, Ruan Q, Fatima A, Getsios S, Lavker RM. MicroRNA-205 promotes keratinocyte migration via the lipid phosphatase SHIP2. *FASEB J* 2010; **24**: 3950–3959.
47 Agueli C, Cammarata G, Salemi D, Dagnino L, Nicoletti R, La Rosa M *et al.* 14q32/miRNA clusters loss of heterozygosity in acute lymphoblastic leukemia is associated with up-regulation of BCL11a. *Am J Hematol* 2010; **85**: 575–578.
48 Ueno K, Hirata H, Majid S, Yamamura S, Shahryari V, Tabatabai ZL *et al.* Tumor suppressor microRNA-493 decreases cell motility and migration ability in human bladder cancer cells by downregulatingRhoC and FZD4. *Mol Cancer Ther* 2012; **11**: 244–253.
49 Peltier HJ, Latham GJ. Normalization of microRNA expression levels in quantitative RT-PCR assays: identification of suitable reference RNA targets in normal and cancerous human solid tissues. *RNA* 2008; **14**: 844–852.
50 Rivetti di Val Cervo P, Lena AM, Nicoloso M, Rossi S, Mancini M, Zhou H *et al.* p63-microRNA feedback in keratinocyte senescence. *Proc Natl Acad Sci USA* 2012; **109**: 1133–1138.

Supplementary Information accompanies this paper on the Oncogene website (http://www.nature.com/onc)